

Enhancing Machine Learning Potentials through Transfer Learning across Chemical Elements

Sebastien Röcken[†] and Julija Zavadlav^{*,†,‡}

[†]*Professorship of Multiscale Modeling of Fluid Materials,*

*Department of Engineering Physics and Computation, TUM School of Engineering and
Design, Technical University of Munich, Germany*

[‡]*Munich Data Science Institute & Munich Institute for Integrated Materials, Energy and
Process Engineering, Technical University of Munich, Germany*

E-mail: julija.zavadlav@tum.de

Abstract

Machine Learning Potentials (MLPs) can enable simulations of ab initio accuracy at orders of magnitude lower computational cost. However, their effectiveness hinges on the availability of considerable datasets to ensure robust generalization across chemical space and thermodynamic conditions. The generation of such datasets can be labor-intensive, highlighting the need for innovative methods to train MLPs in data-scarce scenarios. Here, we introduce transfer learning of potential energy surfaces between chemically similar elements. Specifically, we leverage the trained MLP for silicon to initialize and expedite the training of an MLP for germanium. Utilizing classical force field and ab initio datasets, we demonstrate that transfer learning surpasses traditional training from scratch in force prediction, leading to more stable simulations and improved temperature transferability. These advantages become even more pronounced

as the training dataset size decreases. The out-of-target property analysis shows that transfer learning leads to beneficial but sometimes adversarial effects. Our findings demonstrate that transfer learning across chemical elements is a promising technique for developing accurate and numerically stable MLPs, particularly in a data-scarce regime.

INTRODUCTION

Classical force fields are based on simple, physics-grounded functions, enabling rapid computation of atomic interactions.^{1,2} While they support large-scale Molecular Dynamics simulations, they often fall short in terms of accuracy. In contrast, simulations employing approximative solutions to the Schrödinger equation, such as Density Functional Theory (DFT), offer exceptional precision. Unfortunately, their computational demands render them infeasible to explore the extensive spatiotemporal scales typical of many complex systems.

Machine Learning Potentials (MLPs) have emerged as a powerful tool to reconcile the trade-off between accuracy and computational efficiency.³⁻⁹ The successful applications in literature span diverse systems ranging from alloys^{8,10-13} to biological macromolecules.^{14,15} Trained on DFT data, MLPs can achieve force prediction errors below DFT accuracy¹⁶ while maintaining the ability to simulate million-atom systems.⁵ Despite these promising results, MLPs are inherently limited by the scope of their training datasets and thus require large and informative datasets to yield reliable and accurate models. Various strategies have been proposed to address challenges related to data scarcity.

One widely used approach is active learning,¹⁷⁻¹⁹ where new samples are iteratively selected, labeled, and incorporated into the training dataset. This process is typically driven by uncertainty quantification criteria, allowing models to identify which data points would be most beneficial for training. However, both data labeling and uncertainty quantification can be computationally intensive, especially when employing rigorous Bayesian methods.²⁰ Although non-Bayesian uncertainty quantification techniques^{21,22} may offer viable alterna-

tives with lower computational costs, data labeling remains a notable hurdle in effective active learning implementation.

More recently, there has been a trend towards foundation MLPs,^{15,23–29} where the application domain-unspecific models are built based on extensive datasets comprising a diverse array of chemical elements and compounds. These models can be fine-tuned on a specific chemical sub-space, ideally reducing the required training samples. However, this approach mandates a large-scale neural network to capture the interactions between elements of the entire periodic table, resulting in high computational costs for training and inference. As a result, MLPs tailored to narrower chemical spaces or even focused on individual elements present a more computationally efficient alternative. Nevertheless, utilizing the transfer learning concept, the available databases covering different chemical space than the downstream application can still provide valuable information.

In transfer learning, the knowledge gained from learning one task can be leveraged and transferred to a different but related task.^{30,31} If the transferred knowledge provides useful information, it can enhance data efficiency and accuracy. Therefore, this strategy is particularly advantageous when data for the target task is scarce. Transfer learning has been successfully applied across various domains, from image classification³² to materials discovery.³³ In the context of MLPs, it was used to achieve higher accuracy by pre-training the model on the large DFT dataset and fine-tuning it on the more accurate but smaller coupled cluster dataset.^{34–36} A similar idea is exploited by Δ -Learning, where the difference between a less accurate and a more accurate model is learned.³⁴

Contrary to these previous studies, we propose to employ transfer learning across datasets that span different chemical spaces rather than fine-tuning the model on a chemical sub-space as in foundational models. Our objective is to leverage the knowledge gained while learning the potential energy surface of a chemical element to enhance the learning of another chemical element. Despite the differences in potential energy surfaces among different chemical elements, the fundamental interaction principles—such as steric and van der Waals forces—are

common to all chemical elements. This shared foundation suggests that transfer learning of MLPs across chemical elements could be advantageous, particularly for chemical elements within the same group, as these elements exhibit similar chemical properties. This idea was recently briefly explored by Gardner et al.³⁷ However, since they demonstrate the benefits of transfer learning only for force and energy predictions on synthetically altered data, transfer learning analysis is still missing for other properties and for unaltered real-case dataset scenario.

In this paper, we examine transfer learning of MLPs between chemical elements within the carbon group, specifically between silicon and germanium. Our investigation assesses the advantages of transfer learning across two distinct datasets spanning both solid and liquid phases. The first dataset utilizes the classical Stillinger-Weber potential, which allows for efficient data generation and enables us to rigorously examine the limits of transfer learning. The second dataset is a publicly available DFT dataset, presenting a realistic application scenario. Through our analyses of the Stillinger-Weber dataset, we demonstrate that transfer learning significantly improves the accuracy of force predictions across the solid and liquid bulk regime, as well as enhances the accuracy of phonon density of states (PDOS) in the small dataset regime. Notably, when training models using samples from a single temperature, we observe a marked enhancement in temperature transferability due to transfer learning. In the case of the DFT dataset, transfer learning leads to better force prediction accuracy and more stable simulations compared to the models trained from scratch but does not appear to improve structural properties. Overall, our findings highlight the effectiveness of transfer learning across similar chemical elements as a valuable approach for developing MLPs, especially as a tool to overcome the problems of sparse datasets.

METHODS

In this section, we outline the methodology for training MLPs via force matching and describe the procedure for transfer learning among different chemical elements.

Machine Learning Potential Training via Force Matching

The MLP architecture utilized in this study is a message-passing graph neural network (GNN) DimeNet++.³⁸ This architecture incorporates directional information, which facilitates the inclusion of angular information, thereby enabling precise energy and force predictions. We employ our custom implementation as described in `chemtrain`.³⁹ The embedding size is set to one-quarter of the original, and the cutoff distances are 0.5 nm for Stillinger-Weber data and 0.43 nm for DFT data. The remaining structure adheres to the original implementation.

Different loss functions L can be used to optimize the parameters θ of an MLP.^{40,41} Here, we use the force matching loss

$$L(\theta) = \sum_{j=1}^{N_{bs}} \sum_{k=1}^N \sum_{l=1}^3 \frac{1}{3NN_{bs}} (\hat{F}_{kl}(S_j) - F_{kl}(S_j; \theta))^2, \quad (1)$$

where N_{bs} is the batch size and N is the number of atoms in a configurational state S_j in the batch. \hat{F}_{kl} and F_{kl} denote the target and predicted force on atom k in direction l , respectively. While it is more common to train also on energy labels, we do not use them here to avoid an additional hyperparameter and more complicated analysis. When training only on forces, the energy is determined only up to a constant. We evaluate this constant after the training by calculating the mean energy shift using the training data. The same constant is then used for energy predictions on the test dataset. As detailed in the Supplementary Information, we employ the Adam optimizer with learning rate decay for optimization.

Transfer Learning

The transfer learning of MLPs across different chemical elements follows a two-stage procedure (Figure 1). In the first stage, we pre-train the MLP on a typically large dataset

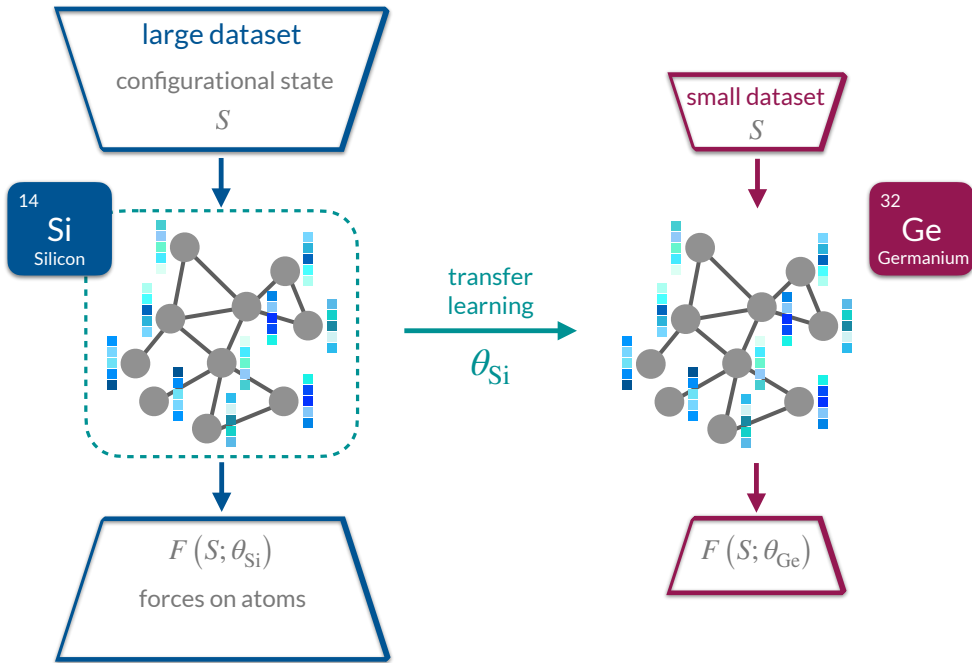


Figure 1: Transfer learning between chemical elements. An MLP is initially trained on a large dataset containing various configurational states \mathbf{S} and corresponding forces on atoms \mathbf{F} for a certain chemical element, here silicon. The resulting parameters θ are then transferred to initialize the parameters of an MLP, which is subsequently trained on a small dataset of a similar but different chemical element, here germanium.

containing different structures and corresponding forces of a particular chemical element (e.g., silicon). In the second stage, we use the obtained parameters to initialize the fine-tuning of an MLP for a similar chemical element (e.g., germanium), for which normally only a limited amount of data is available. We compare the performance of the transfer learning models with those trained from scratch that only undergo the second-stage training using random initialization.

In the transfer learning process, it is possible to freeze some parameters. However, our preliminary analysis showed that the best accuracy is achieved when all parameters are fine-

tuned. Therefore, during the second phase, we retrain all parameters of the MLP for the new chemical element. The employed GNN architecture encodes chemical elements via a learnable atom embedding vector. These embedding parameters are also transferred and retrained during the process.

RESULTS

We evaluate the efficacy of transfer learning MLPs across different chemical elements using Stillinger-Weber and DFT datasets containing bulk silicon or germanium structures. The Stillinger-Weber data serves as a test example due to the simple potential energy surface and the ease of data generation, enabling accurate error estimation due to large test datasets. On the other hand, the DFT data provides a realistic application scenario. In all cases, the direction of knowledge transfer is from silicon to germanium.

SURROGATE MODEL FOR STILLINGER-WEBER POTENTIAL

Dataset

We generate data for silicon and germanium with molecular dynamics simulations at 34 temperatures in the range 300 - 3600 K in 100 K intervals. The molecular interactions are parameterized using a Stillinger-Weber potential following Jian et al.⁴² Simulations of a bulk system comprising 64 atoms are performed in LAMMPS,⁴³ employing a time step of 1 fs, a Nose-Hoover thermostat with a damping factor of 100 time steps, and a Nose-Hoover barostat using a damping factor of 1000 time steps. For each temperature, we conduct a 4 ns NPT equilibration followed by a 1 ns NVT production simulation, sampling every 1 ps. We randomly sample these configurations to create different datasets. For silicon, the train, validation, and test dataset contain, respectively, 20, 5, and 10 samples per temperature or 680, 170, and 340 samples in total. For germanium, we discard the first 100 ps and create a data pool of 30.600 samples (900 per temperature) used for training, validation, and testing.

Data Efficiency

To assess the benefits of alchemical transfer learning, we compare the accuracy of the transfer learning models with models trained from scratch for various training dataset sizes. The transfer learning models are first pre-trained on the silicon dataset. On the test dataset, the silicon MLP model archives very low energy and force mean absolute error (MAE) of 0.127 meV/atom and 0.69 meV/Å, signaling an extensive training data size and a simple target molecular interaction. We then train (re-train in the case of transfer learning) several models on different numbers of samples from the germanium data pool to obtain the germanium MLPs.

In Fig. 2, we report the average MAE of energy and force predictions evaluated on a fixed test dataset containing 340 configurations within the temperature range of 300-3600 K (10 samples per temperature). Transfer learning consistently outperforms training from scratch

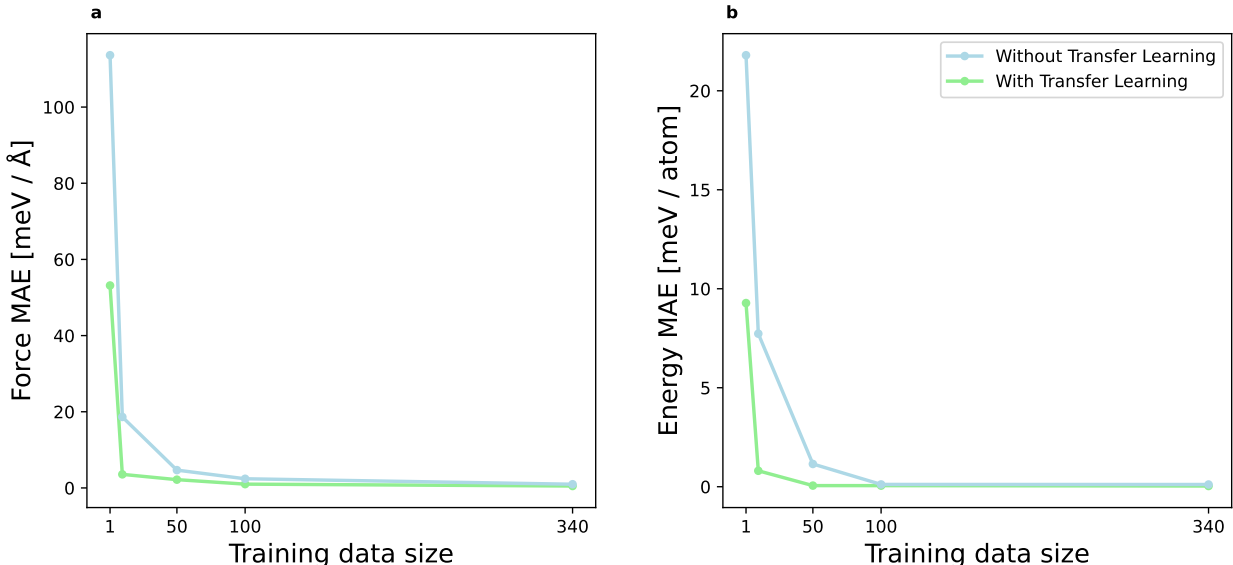


Figure 2: Data efficiency of transfer learning for Stillinger-Weber example. The green and blue lines denote the test set MAE of force (a) and energy (b) predictions for the MLPs trained with and without transfer learning, respectively. The MAE values are averaged over five different models corresponding to different randomly selected train and validation data samples from the data pool. We perform a hyperparameter search for each mode based on the validation dataset (170 samples, 5 per temperature) as reported in the Supplementary Information.

across all training sample sizes. We observe a significant positive transfer learning effect when germanium data is sparse. For example, transfer learning models trained with just 10 samples achieve a lower MAE than models trained from scratch using 50 samples. We attribute this improvement to the similarity in the two underlying potentials and the broad distribution of silicon data. We repeated the analysis also for the solid state samples (see Supplementary Information) and found the same conclusions.

Next, we consider the performance for out-of-target properties and distributions. To achieve this, we further analyze the models trained with just one sample, as these models are already below the chemical accuracy threshold, both with and without transfer learning. Conversely, we will use the best model trained from scratch with the largest dataset of 340 samples as our reference model. At this training data size, the MAEs have converged (Fig. 2), indicating that increasing the training dataset further would not significantly decrease the MAE.

Material Properties

As an out-of-target property, we evaluate the PDOS for MLP models trained on a single random snapshot at 2000 K. These configurations have an amorphous structure even though the temperature is above the germanium melting point due to the inaccuracies of the Stillinger-Weber potential and limited sampling. To compute the PDOS, we generate a 2x2x2 germanium minimum energy super cell with 64 atoms in Avogadro.⁴⁴ For code-specific reasons, we add normally distributed noise $\mathcal{N}(0, 10^{-6})$ nm to the particle positions to avoid exact 180° angles. PDOS is then calculated with phonopy^{45,46} using displacements of 0.01 Å.

The results illustrated in Fig. 3, demonstrate that models utilizing transfer learning closely match the reference MLP that was trained from scratch on a large germanium dataset. In contrast, models that do not use transfer learning show significant differences in PDOS compared to the reference, with notable variations among the five models. This outcome is somewhat expected because the minimum energy configuration differs from the amorphous

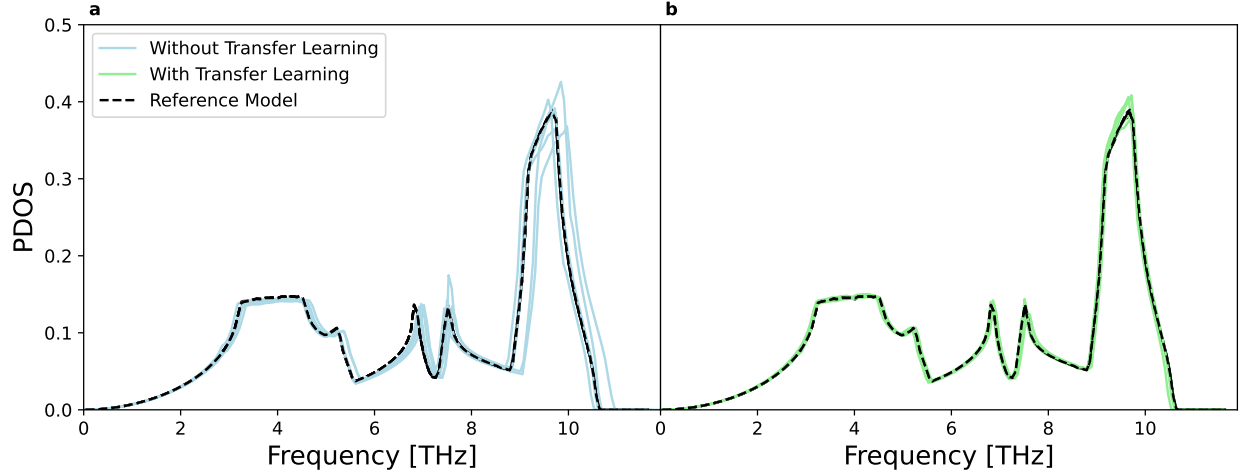


Figure 3: Phonon density of states (PDOS) for Stillinger-Weber example. The results are shown for five models obtained with (b, green) and without (a, blue) transfer learning. These models are trained with a single random sample at 2000 K and compared to the reference germanium model (dashed black) trained on a large dataset containing 340 samples across the entire considered temperature range. The five models correspond to the five best hyperparameter models with different random selections of training and validation data (5 samples at 2000 K).

structure used during (re-)training. The enhanced accuracy observed with transfer learning suggests a successful knowledge transfer for the configurational distribution data gaps.

Temperature Transferability

To further validate this point, we investigate the temperature transferability using the same models as above trained on a single sample at 2000 K. Figure 4 displays the force MAE per atom across test samples generated in the 300-3300 K temperature range. The transfer learning approach delivers significant gains across the entire temperature range. The silicon MLP model initialization, parametrized with samples ranging from 300 to 3600 K, improves the germanium MLP’s performance in temperature regimes not covered by the single germanium training sample. The same outcome is observed also when training on ten samples at 2000 K (see Supplementary Information).

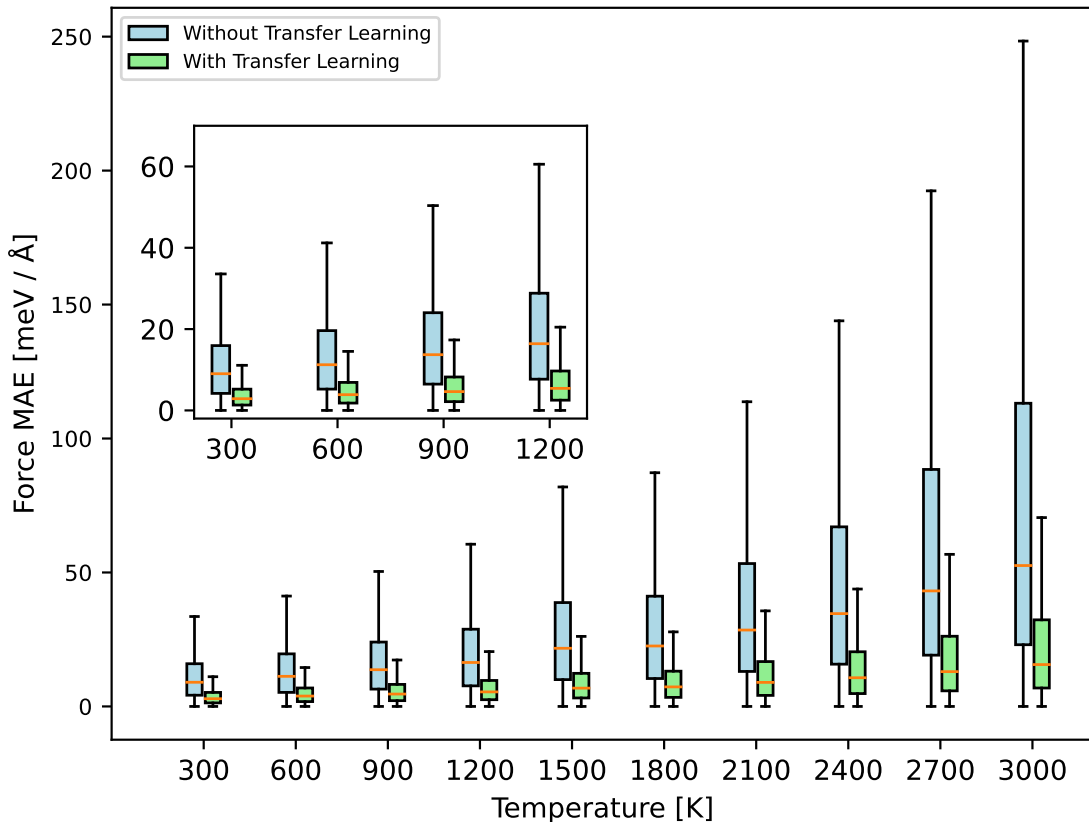


Figure 4: Temperature transferability for Stillinger-Weber example. Transfer learning models (blue) are referenced against the models trained from scratch (green) by computing the force MAE for samples at different temperatures. For both cases, we train five models using a single sample at 2000 K and test each one on 50 samples at the respective temperature, resulting in 250 predictions in total for the 5 models. On the whisker plot, the orange line indicates the median, the box represents the interquartile range (IQR) between the first and third quartiles, and the whiskers extend to the furthest point within 1.5 times the IQR.

DFT SURROGATE MODEL

The results presented thus far were based on data generated using the Stillinger-Weber potential. While this example allowed us to rigorously evaluate performance with extensive test datasets, the Stillinger-Weber potential is relatively simple compared to the more accurate solutions provided by DFT. Thus, we now proceed with a realistic use case by constructing a DFT surrogate model. This model presents an ideal scenario for transfer learning, especially given the challenges associated with generating DFT data.

Dataset

We utilize the DFT dataset for silicon and germanium provided by Zuo et al.⁴⁷ Data includes 2x2x2 bulk structures with deformations up to $\pm 20\%$, single vacancies, and simulation data at temperatures ranging from 300 K to twice the melting temperature (2422 K for germanium and 3374 K for silicon). We exclude the slab structures from the dataset since these are not relevant to our analysis. To avoid exact 180° angles due to code-specific reasons, we add normally distributed noise $\mathcal{N}(0, 10^{-6})$ nm to the particle positions. We partition the silicon data into 182 training samples, 20 validation samples, and 23 test samples. For germanium, 24 samples are set apart for testing, while the remaining 217 samples are used as a data pool for training and validation.

Data Efficiency

We first test the accuracy of the silicon MLP model. We obtain a similar test set accuracy as Zuo et al.,⁴⁷ confirming an expressive enough GNN and an adequate training strategy. In particular, the energy and force root mean squared error (RMSE) are 21.8 meV/atom and 0.10 eV/Å, respectively. Analogous to the Stillinger-Weber example, we proceed with the data efficiency testing of the transfer learning approach by reporting for germanium MLP models the force and energy MAE using 1, 10, 40, 100, and 195 training samples (Fig. 5). Again, we find a significant performance enhancement when employing the transfer learning approach. For the respective training sample sizes, the energy MAE is reduced by 59, 69, 46, 27, -5% and the force MAE by 38, 29, 16, 6, 4%, highlighting positive transfer learning effects for scarce data. With only 10 training samples, the transfer learning models achieve an accuracy below the chemical threshold of 43 meV. In contrast, training from scratch requires all available data (195 samples) to reach chemical accuracy. Note that at this training data size, the MAE of the models with and without transfer learning is very similar and comparable to the errors reported by Zuo et al.⁴⁷

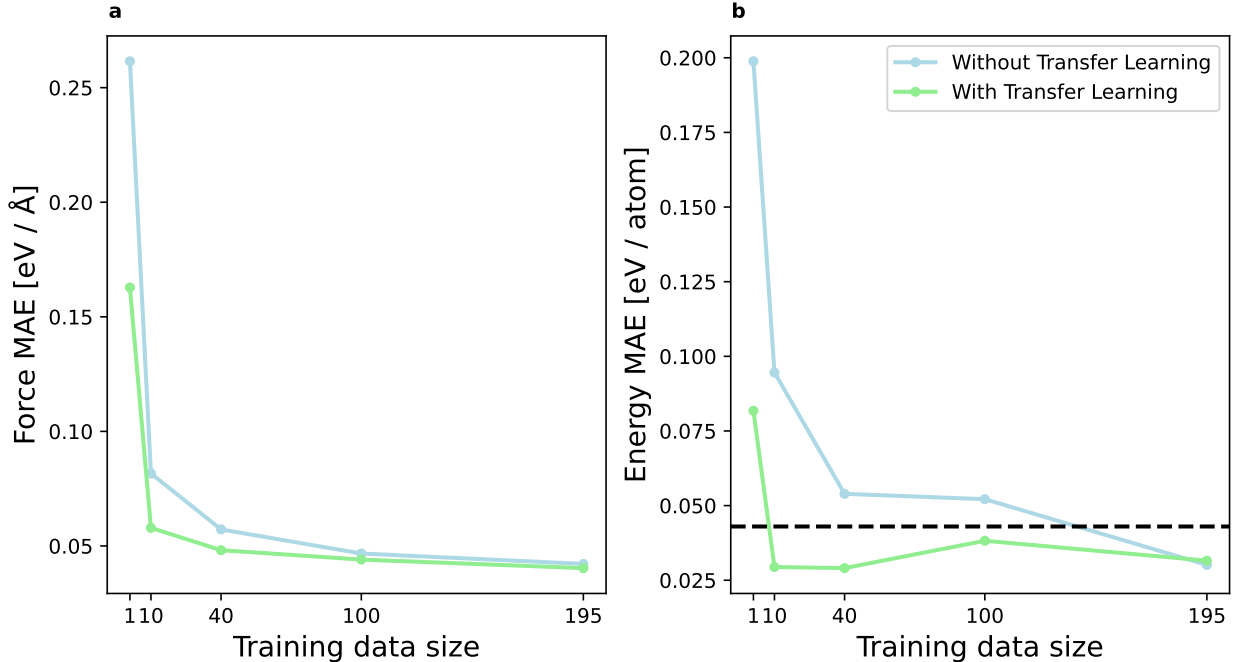


Figure 5: Data efficiency of transfer learning for the DFT example. The green and blue lines denote the test set MAE of force (a) and energy (b) predictions for the MLPs trained with and without transfer learning, respectively. The MAE values are averaged over five different models corresponding to different randomly selected train and validation data samples. We perform a hyperparameter search for each model based on the validation dataset (22 samples) as reported in the Supplementary Information. The black dashed line denotes the chemical accuracy of 43 meV/atom.

Structural Properties

We further assess the impact of transfer learning by examining the structural properties of liquid germanium. In particular, the Radial Distribution Functions (RDFs) and Angular Distribution Functions (ADFs), shown in Fig. 6. The structural properties are evaluated from 100 forward simulations (20 velocity initializations for each of the five models differing in the train/validation data split). The simulations are performed under NVT conditions for 100 ps using the Velocity Verlet integration and a time step of 0.5 fs. The 1200 K temperature is maintained with the Langevin thermostat with a damping coefficient of 1 /ps. All simulations start with the same liquid state configuration in the dataset containing 64 atoms.

With scarce data, the structural properties are not yet fully converged for both ap-

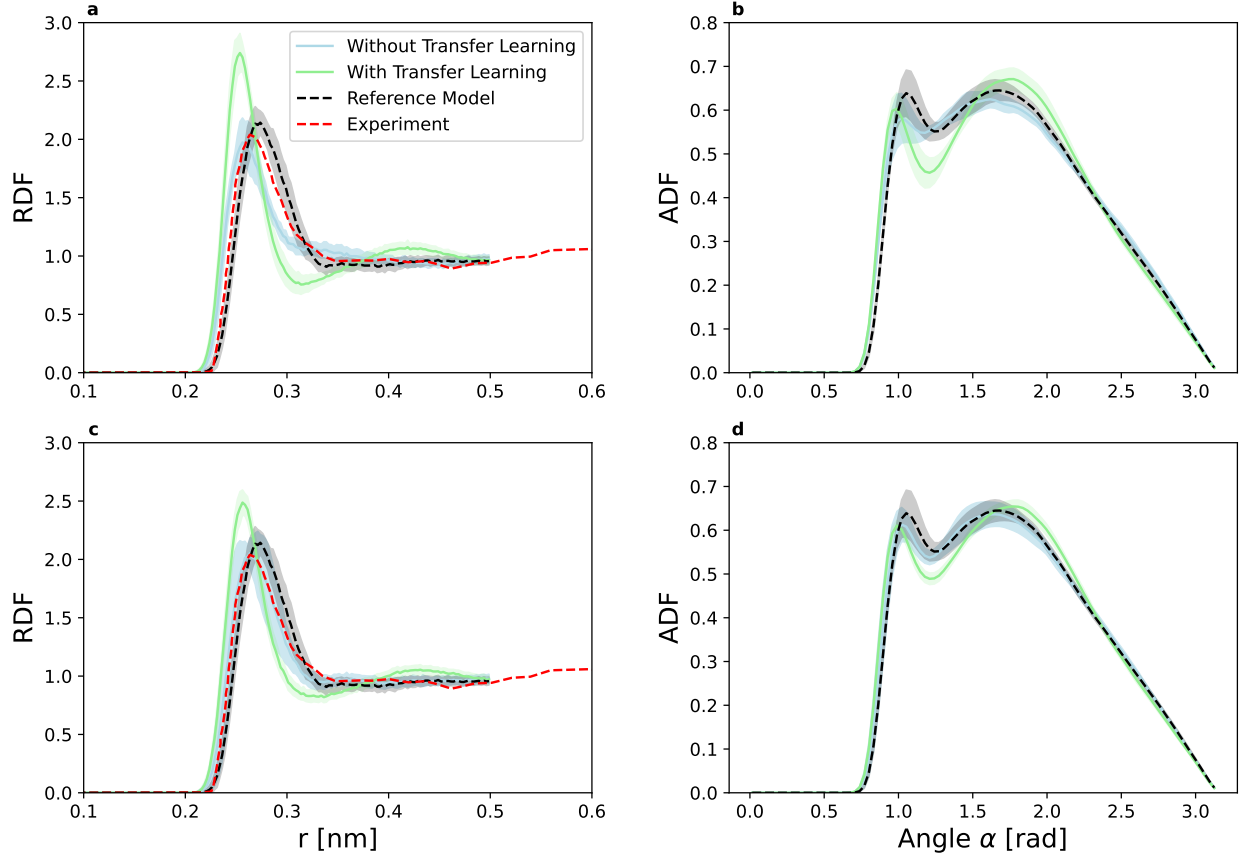


Figure 6: Radial Distribution Function (RDF; left) and Angular Distribution Function (ADF; right) for the DFT example and training data size of 10 (a, b) and 100 (c, d). The green and blue lines denote the models employing transfer learning and the models trained from scratch, respectively. As a reference, we show the results also for the reference model (dashed black), i.e., a germanium MLP trained from scratch with all available data (195 samples). Since some simulation runs resulted in unphysical trajectories, we computed the RDF and ADF from states sampled in the time regime of 10-100 ps, only for models that ran for the full 100 ps and yielded zero RDF values below 0.2 nm. The black solid line represents experimental results from neutron diffraction studies at 1273.15 K.⁴⁸ Shaded regions denote the standard deviation.

proaches—those that use transfer learning and those that do not. Additionally, the RDFs show some deviation from the experimental curve, even with the largest training dataset. This suggests either inaccuracies in DFT calculations or insufficient data. Interestingly, models trained from scratch display a closer alignment with the experimental data, revealing a negative transfer learning effect for the structural properties, despite having lower errors in energy and force predictions. For models that utilize transfer learning, the RDFs and ADFs

gradually shift from the values obtained using the pre-trained silicon model to those derived from the reference germanium model trained from scratch (see Supplementary Information Fig. 3). This finding effectively illustrates the mechanics of transfer learning: the models revert to the pre-trained solution in regions where training data is limited. Although the pre-trained silicon model differs from the target germanium model, it is physically valid and contributes to improved numerical stability, as demonstrated in the following section.

Numerical Stability

Over the past decade, the development of MLPs has advanced significantly. However, numerical stability remains a crucial area that requires improvement.⁴⁹ Specifically, MLPs can display pathological behavior, such as extreme energy and force predictions, resulting in unphysical trajectories characterized by unrealistic bond breaking, particle overlaps, and unstable simulations that may lead to simulation failure.

The stability of MLPs is typically assessed using structural criteria, such as measuring deviations from equilibrium RDFs or equilibrium bond lengths.⁴⁹ In our analysis, we examined 100 forward trajectories used for RDF and ADF computation and evaluated the number of simulations that successfully completed 100 ps without any RDF values falling below 0.2 nm, which signifies no particle overlaps (see Table 1).

Table 1: Numerical Stability of DFT surrogate models with and without transfer learning and various training data sizes. The reported values correspond to the number of successful simulations out of 100 that reached 100 ps without exploding and displaying a zero RDF value below 0.2 nm.

Approach	Training data size			
	10	40	100	195
Without Transfer Learning	35	46	73	71
With Transfer Learning	100	100	80	80

We find that transfer learning significantly improves the numerical stability of MLPs, particularly when working with small training datasets. When conducting forward simulations of liquid germanium using MLPs trained on limited samples, we are likely to encounter

out-of-distribution states. However, by employing transfer learning from a silicon MLP with a broader training data distribution, we can access approximate and physically sound information in these unseen regimes, resulting in more stable behavior. This finding supports our overarching hypothesis that pre-training the model on a chemically similar system allows for the transfer and preservation of information from the pre-training dataset, which is absent from the fine-tuning dataset. The positive impacts of transfer learning are thus most pronounced when there is a significant difference between the distributions of the pre-training and fine-tuning datasets.

CONCLUSIONS

In conclusion, our study highlighted the advantages of the transfer learning technique in the development of MLPs. We built upon the idea that the underlying physical principles governing the interactions of atoms are shared. The more similar two chemical elements are, the closer their potential energy surfaces are likely to be. This reasoning underpins the assumption that transfer learning is beneficial when training MLPs between similar chemical elements. Indeed, we found many benefits of transfer learning MLPs from silicon to germanium, which are closely related and share the same crystal structure. It enables a significantly higher accuracy in force and energy predictions in scenarios with limited training data, supporting the hypothesis that transfer learning among similar chemical elements enhances data efficiency and accuracy. Additionally, we present examples of both positive and negative transfer learning outcomes for other property predictions, allowing for a deeper understanding of the transfer learning mechanism. Importantly, we demonstrate that transfer learning facilitates more stable simulations, suggesting that this approach could play a key role in overcoming numerical stability challenges associated with MLPs.

Data Availability

The data that supports the findings of this study are available within the article and its supplementary material. The code to train presented models will be open-sourced at GitHub: https://github.com/tummfm/TL_MLP.git.

Acknowledgement

This research was funded by the Deutsche Forschungsgemeinschaft (DFG, German Research Foundation) - 534045056. The authors thank Sunny Tamrakar and Frederico Pita de Araujo for their contributions to the initial feasibility studies.

Supporting Information Available

The Supporting Information is available free of charge. Hyperparameter for training on Stillinger-Weber data (Tab. S1); Hyperparameter for training on DFT data (Tab. S2); Data efficiency on test samples in the 300-900 K range for Stillinger-Weber data (Fig. S1); Temperature transferability when training on 10 samples for Stillinger-Weber data (Fig. S2); Structural properties for all transfer learning models on the DFT dataset (Fig. S3).

References

- (1) Vanommeslaeghe, K.; Hatcher, E.; Acharya, C.; Kundu, S.; Zhong, S.; Shim, J.; Darian, E.; Guvench, O.; Lopes, P.; Vorobyov, I., et al. CHARMM general force field: A force field for drug-like molecules compatible with the CHARMM all-atom additive biological force fields. *Journal of computational chemistry* **2010**, *31*, 671–690.
- (2) Wang, J.; Wolf, R. M.; Caldwell, J. W.; Kollman, P. A.; Case, D. A. Development and

- testing of a general amber force field. *Journal of computational chemistry* **2004**, *25*, 1157–1174.
- (3) Schütt, K. T.; Sauceda, H. E.; Kindermans, P.-J.; Tkatchenko, A.; Müller, K.-R. Schnet—a deep learning architecture for molecules and materials. *The Journal of Chemical Physics* **2018**, *148*.
 - (4) Batzner, S.; Musaelian, A.; Sun, L.; Geiger, M.; Mailoa, J. P.; Kornbluth, M.; Molinari, N.; Smidt, T. E.; Kozinsky, B. E (3)-equivariant graph neural networks for data-efficient and accurate interatomic potentials. *Nature communications* **2022**, *13*, 2453.
 - (5) Musaelian, A.; Batzner, S.; Johansson, A.; Sun, L.; Owen, C. J.; Kornbluth, M.; Kozinsky, B. Learning local equivariant representations for large-scale atomistic dynamics. *Nature Communications* **2023**, *14*, 579.
 - (6) Behler, J.; Parrinello, M. Generalized neural-network representation of high-dimensional potential-energy surfaces. *Physical review letters* **2007**, *98*, 146401.
 - (7) Duval, A. A.; Schmidt, V.; Hernández-García, A.; Miret, S.; Malliaros, F. D.; Bengio, Y.; Rolnick, D. Faenet: Frame averaging equivariant gnn for materials modeling. International Conference on Machine Learning. 2023; pp 9013–9033.
 - (8) Röcken, S.; Zavadlav, J. Accurate machine learning force fields via experimental and simulation data fusion. *npj Computational Materials* **2024**, *10*, 69.
 - (9) Röcken, S.; Burnet, A. F.; Zavadlav, J. Predicting solvation free energies with an implicit solvent machine learning potential. *The Journal of Chemical Physics* **2024**, *161*.
 - (10) Bartók, A. P.; Kermode, J.; Bernstein, N.; Csányi, G. Machine learning a general-purpose interatomic potential for silicon. *Physical Review X* **2018**, *8*, 041048.
 - (11) Wen, T.; Wang, R.; Zhu, L.; Zhang, L.; Wang, H.; Srolovitz, D. J.; Wu, Z. Specialising

- neural network potentials for accurate properties and application to the mechanical response of titanium. *npj Computational Materials* **2021**, 7, 206.
- (12) Rowe, P.; Csányi, G.; Alfe, D.; Michaelides, A. Development of a machine learning potential for graphene. *Physical Review B* **2018**, 97, 054303.
 - (13) Andolina, C. M.; Saidi, W. A. Highly transferable atomistic machine-learning potentials from curated and compact datasets across the periodic table. *Digital Discovery* **2023**, 2, 1070–1077.
 - (14) Merchant, A.; Batzner, S.; Schoenholz, S. S.; Aykol, M.; Cheon, G.; Cubuk, E. D. Scaling deep learning for materials discovery. *Nature* **2023**, 624, 80–85.
 - (15) Takamoto, S.; Shinagawa, C.; Motoki, D.; Nakago, K.; Li, W.; Kurata, I.; Watanabe, T.; Yayama, Y.; Iriguchi, H.; Asano, Y., et al. Towards universal neural network potential for material discovery applicable to arbitrary combination of 45 elements. *Nature Communications* **2022**, 13, 2991.
 - (16) Faber, F. A.; Hutchison, L.; Huang, B.; Gilmer, J.; Schoenholz, S. S.; Dahl, G. E.; Vinyals, O.; Kearnes, S.; Riley, P. F.; von Lilienfeld, O. A. Machine learning prediction errors better than DFT accuracy. *arXiv preprint arXiv:1702.05532* **2017**,
 - (17) Smith, J. S.; Nebgen, B.; Lubbers, N.; Isayev, O.; Roitberg, A. E. Less is more: Sampling chemical space with active learning. *The Journal of chemical physics* **2018**, 148.
 - (18) Thaler, S.; Mayr, F.; Thomas, S.; Gagliardi, A.; Zavadlav, J. Active learning graph neural networks for partial charge prediction of metal-organic frameworks via dropout Monte Carlo. *npj Computational Materials* **2024**, 10, 86.
 - (19) Zhang, L.; Lin, D.-Y.; Wang, H.; Car, R.; E, W. Active learning of uniformly accurate interatomic potentials for materials simulation. *Physical Review Materials* **2019**, 3, 023804.

- (20) Thaler, S.; Doehner, G.; Zavadlav, J. Scalable Bayesian uncertainty quantification for neural network potentials: promise and pitfalls. *Journal of Chemical Theory and Computation* **2023**, *19*, 4520–4532.
- (21) Kellner, M.; Ceriotti, M. Uncertainty quantification by direct propagation of shallow ensembles. *Machine Learning: Science and Technology* **2024**,
- (22) Bigi, F.; Chong, S.; Ceriotti, M.; Grasselli, F. A prediction rigidity formalism for low-cost uncertainties in trained neural networks. *arXiv preprint arXiv:2403.02251* **2024**,
- (23) Takamoto, S.; Izumi, S.; Li, J. TeaNet: Universal neural network interatomic potential inspired by iterative electronic relaxations. *Computational Materials Science* **2022**, *207*, 111280.
- (24) Batatia, I.; Benner, P.; Chiang, Y.; Elena, A. M.; Kovács, D. P.; Riebesell, J.; Advincula, X. R.; Asta, M.; Baldwin, W. J.; Bernstein, N., et al. A foundation model for atomistic materials chemistry. *arXiv preprint arXiv:2401.00096* **2023**,
- (25) Allen, A. E.; Lubbers, N.; Matin, S.; Smith, J.; Messerly, R.; Tretiak, S.; Barros, K. Learning together: Towards foundation models for machine learning interatomic potentials with meta-learning. *npj Computational Materials* **2024**, *10*, 154.
- (26) Zhang, D.; Liu, X.; Zhang, X.; Zhang, C.; Cai, C.; Bi, H.; Du, Y.; Qin, X.; Peng, A.; Huang, J., et al. DPA-2: a large atomic model as a multi-task learner. *npj Computational Materials* **2024**, *10*, 293.
- (27) Shoghi, N.; Kolluru, A.; Kitchin, J. R.; Ulissi, Z. W.; Zitnick, C. L.; Wood, B. M. From molecules to materials: Pre-training large generalizable models for atomic property prediction. *arXiv preprint arXiv:2310.16802* **2023**,
- (28) Yang, H.; Hu, C.; Zhou, Y.; Liu, X.; Shi, Y.; Li, J.; Li, G.; Chen, Z.; Chen, S.; Zeni, C.,

- et al. Mattersim: A deep learning atomistic model across elements, temperatures and pressures. *arXiv preprint arXiv:2405.04967* **2024**,
- (29) Kolluru, A.; Shoghi, N.; Shuaibi, M.; Goyal, S.; Das, A.; Zitnick, C. L.; Ulissi, Z. Transfer learning using attentions across atomic systems with graph neural networks (TAAG). *The Journal of Chemical Physics* **2022**, *156*.
 - (30) Zhuang, F.; Qi, Z.; Duan, K.; Xi, D.; Zhu, Y.; Zhu, H.; Xiong, H.; He, Q. A comprehensive survey on transfer learning. *Proceedings of the IEEE* **2020**, *109*, 43–76.
 - (31) Pan, S. J.; Yang, Q. A survey on transfer learning. *IEEE Trans. Knowl. Data Eng.* **2009**, *22*, 1345–1359, DOI: 10.1109/TKDE.2009.191.
 - (32) Oquab, M.; Bottou, L.; Laptev, I.; Sivic, J. Learning and transferring mid-level image representations using convolutional neural networks. Proceedings of the IEEE conference on computer vision and pattern recognition. 2014; pp 1717–1724, DOI: 10.1109/CVPR.2014.222.
 - (33) Feng, S.; Fu, H.; Zhou, H.; Wu, Y.; Lu, Z.; Dong, H. A general and transferable deep learning framework for predicting phase formation in materials. *Npj Computational Materials* **2021**, *7*, 1–10, DOI: 10.1038/s41524-020-00488-z.
 - (34) Dral, P. O.; Zubatiuk, T.; Xue, B.-X. *Quantum Chemistry in the Age of Machine Learning*; Elsevier, 2023; pp 491–507.
 - (35) Smith, J. S.; Nebgen, B. T.; Zubatyuk, R.; Lubbers, N.; Devereux, C.; Barros, K.; Tretiak, S.; Isayev, O.; Roitberg, A. E. Approaching coupled cluster accuracy with a general-purpose neural network potential through transfer learning. *Nature communications* **2019**, *10*, 2903.
 - (36) Zaverkin, V.; Holzmüller, D.; Bonferraro, L.; Kästner, J. Transfer learning for chemically

- accurate interatomic neural network potentials. *Physical Chemistry Chemical Physics* **2023**, *25*, 5383–5396.
- (37) Gardner, J. L.; Baker, K. T.; Deringer, V. L. Synthetic pre-training for neural-network interatomic potentials. *Machine Learning: Science and Technology* **2024**, *5*, 015003.
- (38) Gasteiger, J.; Giri, S.; Margraf, J. T.; Günnemann, S. Fast and uncertainty-aware directional message passing for non-equilibrium molecules. *arXiv preprint arXiv:2011.14115* **2020**,
- (39) Fuchs, P.; Thaler, S.; Röcken, S.; Zavadlav, J. chemtrain: Learning deep potential models via automatic differentiation and statistical physics. *Computer Physics Communications* **2025**, 109512.
- (40) Thaler, S.; Zavadlav, J. Learning neural network potentials from experimental data via Differentiable Trajectory Reweighting. *Nature communications* **2021**, *12*, 6884.
- (41) Thaler, S.; Stupp, M.; Zavadlav, J. Deep Coarse-Grained Potentials via Relative Entropy Minimization. *The Journal of Chemical Physics* **2022**, *157*, 244103.
- (42) Jian, Z.; Kaiming, Z.; Xide, X. Modification of stillinger-weber potentials for si and ge. *Physical Review B* **1990**, *41*, 12915.
- (43) Thompson, A. P.; Aktulga, H. M.; Berger, R.; Bolintineanu, D. S.; Brown, W. M.; Crozier, P. S.; in 't Veld, P. J.; Kohlmeyer, A.; Moore, S. G.; Nguyen, T. D.; Shan, R.; Stevens, M. J.; Tranchida, J.; Trott, C.; Plimpton, S. J. LAMMPS - a flexible simulation tool for particle-based materials modeling at the atomic, meso, and continuum scales. *Computer Physics Communication* **2022**, *271*, 108171.
- (44) Hanwell, M. D.; Curtis, D. E.; Lonie, D. C.; Vandermeersch, T.; Zurek, E.; Hutchison, G. R. Avogadro: an advanced semantic chemical editor, visualization, and analysis platform. *Journal of cheminformatics* **2012**, *4*, 1–17.

- (45) Togo, A.; Chaput, L.; Tadano, T.; Tanaka, I. Implementation strategies in phonopy and phono3py. *Journal of Physics: Condensed Matter* **2023**, *35*, 353001.
- (46) Togo, A. First-principles Phonon Calculations with Phonopy and Phono3py. *Journal of the Physical Society of Japan* **2023**, *92*, 012001.
- (47) Zuo, Y.; Chen, C.; Li, X.; Deng, Z.; Chen, Y.; Behler, J.; Csányi, G.; Shapeev, A. V.; Thompson, A. P.; Wood, M. A., et al. Performance and cost assessment of machine learning interatomic potentials. *The Journal of Physical Chemistry A* **2020**, *124*, 731–745.
- (48) Salmon, P. A neutron diffraction study on the structure of liquid germanium. *Journal of Physics F: Metal Physics* **1988**, *18*, 2345.
- (49) Fu, X.; Wu, Z.; Wang, W.; Xie, T.; Keten, S.; Gomez-Bombarelli, R.; Jaakkola, T. Forces are not enough: Benchmark and critical evaluation for machine learning force fields with molecular simulations. *arXiv preprint arXiv:2210.07237* **2022**,

TOC Graphic

